# GROWTH AND CHARACTERIZATION OF INDIUM OXIDE NANOSTRUCTURED FILMS USING SOLID-TO-VAPOR DEPOSITION TECHNIQUE FOR PHOTOELECTROCHEMICAL APPLICATIONS

**APER TERWASE MOSES**

**UNIVERSITI SAINS MALAYSIA**

**2022**

# GROWTH AND CHARACTERIZATION OF INDIUM OXIDE NANOSTRUCTURED FILMS USING SOLID-TO-VAPOR DEPOSITION TECHNIQUE FOR PHOTOELECTROCHEMICAL APPLICATIONS

**by**

**APER TERWASE MOSES**

**Thesis submitted in fulfillment of the requirements**
**for the degree of**
**Doctor of Philosophy**

**May 2022**

# ACKNOWLEDGEMENT

With all sense of humility, I give God Almighty glory, honor, and praise for seeing me through this research work. I wish to express my unreserved gratitude and appreciation to my main supervisor, Assoc. Professor Dr. Fong Kwong Yam for his valuable suggestions and ideas and his uncommon patience in guidance and motivating me throughout the research period. I sincerely appreciate my co-supervisor, Dr. Khi Poay Beh, for his helpful suggestions that have contributed significantly to the success of this research work. I thank all the lab technicians and staff of Nano Optoelectronics Research Laboratory (NOR-Lab), USM, for their technical support in handling research equipment.

I want to express my profound gratitude to the government of the Federal Republic of Nigeria through the Tertiary Education Trust Fund (TETFund) and Benue State University, Makurdi, Nigeria, for the financial support given to me throughout this research. I sincerely appreciate this gesture, and I pray God to give me the grace to use the knowledge acquired to contribute to the development of our dear country.

My special thanks go to my dear wife Mimi and my lovely children: Yimam, Iengem, Tsegham, Ungumimi, and Ukuram. You have been the source of strength that keeps pushing me not to give up. I cannot appreciate you enough. Finally, I also appreciate my aged mother, Mama Nauman, and my siblings for your prayers and encouragement. May God bless us all.

Thank you.

Aper Terwase Moses.

## TABLE OF CONTENTS

## LIST OF TABLES

**Page**

## LIST OF FIGURES

**Page**

## LIST OF SYMBOLS

| | |
|---|---|
| $\alpha$ | Absorption coefficient |
| $\eta$ | Apply bias to photon conversion efficiency (ABPE) |
| K | Boltzmann constant |
| $\Theta$ | Bragg diffraction angle |
| $e_0 N_D$ | Carrier density |
| $R_{ct}$ | Charge transfer resistance |
| CP | Interfacial capacitance |
| A | Cross-sectional area |
| D | Crystallite size |
| $^oC$ | Degree centigrade |
| $T_D$ | Deposition temperature |
| $\varepsilon$ | Dielectric constant of semiconductor |
| $\delta$ | dislocation density |
| eV | Electron volt |
| $e_0$ | Electronic charge |
| $E_F$ | Fermi energy |
| $\nu$ | Frequency |
| $\beta$ | Full width at half maximum |
| $V_{fb}$ | Flat band potential |
| $Z_{imag}$ | Imaginary impedance |
| C | Interfacial capacitance |
| h,k,l | Miller indices |
| $\Omega$ | Ohm |
| $V_{on}$ | Onset potential |
| $E_g$ | Optical bandgap |

| | |
|---|---|
| $V_0$ | Oxygen Vacancies |
| $\varepsilon_0$ | Permittivity of free space |
| $J_{phot}$ | Photocurrent density |
| $h$ | Planck constant |
| $\Delta\varphi_{SC}$ | Potential drop across depletion layer |
| $J_{light}$ | Power density of incident light |
| $Z_{real}$ | Real impedance |
| $R_b$ | Resistance in the bulk of semiconductor material |
| $R_s$ | Resistance of solution |
| $\varepsilon$ | Strain |
| T | Temperature |
| W | Watt |
| $\lambda$ | Wavelength |
| $\omega$ | width of depletion layer |

## LIST OF ABBREVIATIONS

| | |
|---|---|
| ABPE | Applied Bias Photon-to-current Efficiency |
| AC | Alternating Current |
| Ag/AgCl | Silver by Silver Chloride |
| APCE | Absorbed Photon-to-current Conversion Efficiency |
| BCC | Body Centered Cubic |
| CB | Conduction Band |
| CBD | Chemical Bath Deposition |
| $CH_4$ | Methane |
| $C_2H_6$ | Ethane |
| CPE | Constant Phase Element |
| CO | Carbon Monoxide |
| $CO_2$ | Carbon Dioxide |
| $Co_3O_3$ | Cobalt Oxide |
| $Cu_2O$ | Copper Oxide |
| CVD | Chemical Vapour Deposition |
| DC | Direct Current |
| DFT | Density Functional Theory |
| DI | Deionized Water |
| EDX | Energy Dispersive X-ray Spectroscopy |
| EIS | Electrochemical Impedance Spectroscopy |
| $Fe_2O_3$ | Iron(III) Oxide |
| FET | Field Emission Transistor |
| FTO | Fluorine-doped Tin Oxide |
| FESEM | Field Emission Scanning Electron Microscope |
| $Ga_2O_3$ | Gallium Oxide |

| | |
|---|---|
| Gb-In-Zn | Gadolinium-Indium-Zinc Oxide |
| HRCVD | Hydrogen-Reduction Chemical Vapour Deposition |
| HER | Hydrogen Evolution Reaction |
| $In^{+3}$ | Indium Ion |
| In(BTC)(Phen)($H_2O$) | Biphenyi-2,4-Tricarboxylic Acid |
| $In_2O_3$ | Indium Oxide |
| $In(OH)_3$ | Indium Hydroxide |
| IPCE | Incident Photon to current Conversion Efficiency |
| ITO | Indium-doped Tin Oxide |
| JCPDS | Joint Committee on Power Diffraction Standards |
| K-M | Kubelka-Munk theory |
| KOH | Potassium Hydroxide |
| LSV | Linear Sweep Voltammetry |
| MBE | Molecular Beam Epitaxy |
| MgO | Magnesium Oxide |
| MOS | Metal Oxide Semiconductor |
| M-S | Mott-Schottky |
| NHE | Normal Hydrogen Electrode |
| nm | Nanometre |
| OER | Oxygen Evolution Reaction |
| OIE | Oxygen Isotope Equilibration |
| OVRU | Oxygen-Vacancy-Rich Ultrathin |
| PEC | Photoelectrochemical |
| PFOA | Perfluoroctanoic Acid |
| PhO | Photo-oxidation |
| PV | Photovoltaic |
| RhB | Rhodamine-B |

| | |
|---|---|
| $R_2O_3$ | Rare earth sesquioxides |
| RWGS | Reverse Water Gas Shift |
| SC | Semiconductor |
| Sccm | Standard cubic centimeters per min |
| SCL | Space-Charge Layer |
| SCLJ | Semiconductor Liquid Junction |
| $SnO_2$ | Tin Oxide |
| SiNW | Silicon Nanowires |
| STH | Solar to Hydrogen |
| STO | Solar to Oxygen |
| SVD | Solid-to-vapor deposition |
| TCO | Transparent Conducting Oxide |
| Ti-$Fe_2O_3$ | Titanium-iron (III) Oxide |
| $TiO_2$ | Titanium dioxide |
| UV-Vis | Ultraviolet-Visible Spectroscopy |
| VB | Valence Band |
| VLS | Vapor Liquid Solid |
| VS | Vapor Solid |
| $WO_3$ | Tungsten Oxide |
| XRD | X-ray Diffraction |
| ZnO | Zinc Oxide |
| 1D | One Dimension |
| 2D | Two Dimension |
| 3D | Three Dimension |

## LIST OF APPENDICES

**PERTUMBUHAN DAN PENCIRIAN FILEM NANOSTRUKTUR INDIUM OKSIDA MENGGUNAKAN TEKNIK PEMENDAPAN PEPEJAL KE WAP UNTUK APLIKASI FOTOELEKTROKIMIA**

## ABSTRAK

Penyelidikan ini menyelidiki sifat morfologi, struktur, optik, dan fotolistrik dari filem nanostruktur $In_2O_3$ yang disintesis pada substrat Si(100) dan Ni/Si(100) menggunakan teknik pemendapan wap kimia pada tekanan atmosfera di bawah ambien penurun hidrogen, dan karbotermal, masing-masing. Sifat-sifat filem yang disintesis dikaji dalam beberapa keadaan pertumbuhan seperti; suhu, kadar aliran gas, dan penyepuhlindapan di bawah ambien amonia. Analisis menunjukkan perubahan morfologi permukaan filem dengan variasi keadaan pertumbuhan. Pengukuran EDX menunjukkan bukan stoikiometrik dalam semua filem dengan nisbah atom In/O di atas nilai stoikiometrik 0.667, yang menunjukkan kekurangan oksigen. Analisis XRD mengesahkan pembentukan struktur nano oksida indium oksida yang sangat berkristal dari struktur kristal kubik (bcc) berpusat badan dengan pertumbuhan mendominasi pada bidang (222). Sampel variasi jalur optik dengan keadaan pertumbuhan juga diperhatikan dari analisis data pantulan. Penyepuhan di bawah ambien amonia mengakibatkan pembentukan bahan berstruktur nano $In_2O_3$ terdop-N. Kajian fotoelektrokimia menunjukkan potensi permulaan 0.72 (V vs Ag/AgCl) untuk arus fotoanodik dalam elektrod yang dibuat di bawah ambien penurun hidrogen yang dengan fotoanod yang paling cekap (dibuat pada suhu 950 $^oC$), menghasilkan kepadatan arus foto maksimum 2.56 ($mA/cm^2$). Elektrod foto N- $In_2O_3$, sebaliknya, mencatatkan potensi permulaan 0.18 (V vs Ag/AgCl) untuk penjanaan arus foto.

Ketumpatan arus foto diperhatikan meningkat dengan peningkatan pendopan-N, seperti yang disimpulkan dari analisis EDX. Elektrod dengan kepekatan N- tertinggi menunjukkan ketumpatan arus foto maksimum 1.33 ($mA/cm^2$), kira-kira tiga kali lebih besar daripada elektrod intrinsik. Peningkatan aktiviti fotoanodik dalam elektrod disebabkan oleh beberapa faktor mulai dari peningkatan kekristalan seperti yang ditentukan oleh analisis XRD, luas permukaan yang besar disimpulkan dari ketumpatan bahan dalam sampel, dan penyempitan jurang jalur. Peningkatan prestasi foto juga disebabkan oleh peningkatan kepekatan pembawa cas seperti yang ditentukan oleh analisis Mott-Schottky. Secara keseluruhan, hasilnya menunjukkan bahawa filem berstruktur nano $In_2O_3$ yang disintesis dengan teknik CVD di bawah persekitaran pengurangan hidrogen dan pendop-N $In_2O_3$ yang disintesis oleh CVD adalah cara yang mungkin untuk memperbaiki sifat filem $In_2O_3$ untuk aplikasi pemisahan air. Hasil kajian juga menunjukkan bahawa keseimbangan Ni dan 1% $H_2$, $N_2$ adalah pemangkin berpotensi dan gas pembawa, masing-masing, untuk sintesis CVD filem nano kristal berhasil tinggi $In_2O_3$.

**GROWTH AND CHARACTERIZATION OF INDIUM OXIDE NANOSTRUCTURED FILMS USING SOLID-TO-VAPOR DEPOSITION TECHNIQUE FOR PHOTOELECTROCHEMICAL APPLICATIONS**

## ABSTRACT

This research investigates the morphological, structural, optical, and photoelectrochemical properties of $In_2O_3$ nanostructured films synthesized on Si(100) and Ni/Si(100) substrates using the chemical vapor deposition technique at atmospheric pressure under hydrogen reducing ambient, and carbothermal reduction, respectively. The properties of the synthesized films were studied under several growth conditions such as; temperature, gas flow rates, and post-annealing under ammonia ambient. Analysis revealed changes in the surface morphology of the films with variations in growth conditions. EDX measurements showed non-stoichiometric in all the films with an In/O atomic ratio above the stoichiometric value of 0.667, which indicates oxygen deficiency. XRD analysis confirmed the formation of highly crystalline indium oxide nanostructures of the body-centered cubic (bcc) crystal structure with predominate growth in the (222) plane. Samples optical bandgap variation with growth conditions was also observed from analysis of reflectance data. Annealing under ammonia ambient resulted in the formation of N-doped $In_2O_3$ nanostructured materials. The photoelectrochemical study performed in a 0.5 M KOH solution revealed an onset potential of 0.72 (V vs. Ag/AgCl) for photoanodic current in the electrodes fabricated under hydrogen reducing ambient with the most efficient photoanode (fabricated at 950 $^oC$), generating a maximum photocurrent density of 2.56 ($mA/cm^2$). The N-$In_2O_3$ photoelectrodes, on the other hand, recorded an onset potential

of 0.18 (V vs. Ag/AgCl) for photocurrent generation. The photocurrent density was observed to increase with increasing N-doping, as inferred from the EDX analysis. The electrode with the highest N-concentration exhibits a maximum photocurrent density of 1.33 ($mA/cm^2$), about three times larger than 0.43 ($mA/cm^2$) generated by the intrinsic electrode. The enhanced photoanodic activity in the electrodes was attributed to several factors ranging from enhanced crystallinity as determined by XRD analysis, large surface area as deduced from the density of material in samples, and bandgap narrowing. Improved photo-performance was also ascribed to enhanced charge carrier concentration as determined by Mott-Schottky analysis. Overall, the result demonstrates that $In_2O_3$ nanostructured films synthesized by CVD technique under hydrogen reducing environment and N-doping of $In_2O_3$ synthesized by CVD are possible ways of improving the properties of $In_2O_3$ films for water splitting application. The work also revealed that Ni and 1 % $H_2$ balance $N_2$ is a potential catalyst and carrier gas, respectively, for the CVD synthesis of high yield $In_2O_3$ nanocrystalline films.

# CHAPTER 1

# INTRODUCTION

## 1.1 Introduction

Low dimensional metal oxide semiconductors (MOS) have received intense research attention because of their excellent optical and electrical properties that are attractive for technological and scientific applications. Typical binary oxides such as $Ga_2O_3$, $In_2O_3$, $SnO_2$, $TiO_2$, and ZnO have been extensively studied and applied in various aspects of modern devices, including electronic, optical, magnetic, and catalytic applications [1–5]. Specifically, the oxides materials play an essential role in energy storage, dielectric, optoelectronic, ferroelectric, spintronic, and biosensors materials [6–12]. A combination of high reflectance in the infrared region and high transparency in the visible region is a crucial property that has made the oxides useful in architectural windows application.

Indium oxide ($In_2O_3$) is one fascinating MOS material with n-type conductivity. It has been well studied over the years for numerous applications in optoelectronics and nanoelectronics devices [13]. When doped with tin oxide ($SnO_2$), it forms tin-doped indium oxide (ITO), a typical material commonly referred to as transparent conducting oxide (TCO) [14]. $In_2O_3$ nanostructures have been investigated for a range of applications, including sensors [15], photodetectors [16], solar cells [17], field emission transistors (FET) [18], and photocatalysis [19], among others. The importance of this material is derived from its unique characteristics such as wide bandgap (≈3.0-3.75 eV), high transparency in the visible region of the electromagnetic spectrum, low resistivity, and high chemical stability [20,21].

Single crystal of $In_2O_3$ was first prepared by Remeika and Spencer in 1964 using a flux technique for electrical conductivity measurements [22]. Since then, $In_2O_3$ nanoparticles, thin films, and nanostructured films have been prepared by many groups through several synthesis techniques such as hydrothermal, thermal evaporation, sol-gel spin coating, spray pyrolysis, sputtering, molecular beam epitaxy (MBE), pulsed laser ablation, and chemical vapor deposition (CVD) [23–29]. Depending on the synthesis technique employed and the growth parameters, $In_2O_3$ films with varying morphological, structural, optical, and electrical properties for functional device applications have been widely reported in the literature.

Many researchers have adopted the vapor transport synthesis technique in preparing $In_2O_3$ nanostructures with high crystalline quality. The vapor route synthesis technique offers an opportunity to synthesize nanostructures of diverse morphologies through the modulation of various experimental conditions, such as precursor, gas flow, source temperature. Among the vapor route deposition techniques, the CVD process has proven to be effective in fabricating low-dimensional nanostructured indium oxide films with interesting properties for potential applications in nanotechnology [30,31]. Many authors have reported on the CVD synthesis of $In_2O_3$ nanostructures through the vapor-solid (VS) and vapor-liquid-solid (VLS) growth mechanisms. The morphology and structure of material have been known to play a crucial role in determining its physical properties. Miniaturization of material over the years has led to the discovery of novel properties that have greatly influenced modern-day nanoscience and nanotechnological advancement. There is, therefore, a need for continuous synthesis and property evaluation of materials such as $In_2O_3$ for future device applications.

To date, the global energy supply is heavily dependent on non-renewable and depleting sources such as fossil fuels [32]. However, the high energy consumption rate due to population growth, urbanization, and industrialization raises concerns for the sustainable supply of energy from these sources. Environmental and health challenges arising from the accumulation of greenhouse gases in the atmosphere, resulting from the continuous use of these forms of energy, are another issue the world is facing [33,34]. Hence the need for alternative sources of energy.

Solar energy is an abundant energy source with the capacity to generate in excess the global energy consumption requirements [35]. In recent decades, there have been increasing research activities to develop photovoltaic (PV) devices that can convert sunlight into electricity as an alternative way in replacing fossil fuels. Although significant achievement has been made, there is a storage-related problem as the available storage systems are of small capacity, hence the need for largescale energy storage solutions. The generation of chemical fuels using solar energy can overcome the energy storage problem [36].

Hydrogen is a potential clean energy source since the energy density is higher than fossil fuels, and water is the by-product of its combustion process [37]. Currently, $H_2$ is mainly produced from catalytic cracking of hydrocarbons but, it can also be obtained through sustainable methods. Solar water splitting is a chemical reaction driven by photons in which water molecules are broken down into constituent elements (H and O). Absorption of light and dissociation of water are the important steps involved in this process, which can be performed separately or at the same time. In the first instance, the system acts as an electrolyzer, where solar energy is converted into electricity by a solar cell, which is then used to power water electrolysis. In the second case, a photoactive semiconductor material is made to absorb photons from the solar

spectrum and generate charge carriers, which are then utilized to activate the redox reaction for hydrogen evolution [38–40].

Photoelectrodes are employed in Photoelectrochemical (PEC) cells for water splitting reactions. In this configuration, charge transfer processes occur at a semiconductor/liquid junction [41]. A good photoelectrode semiconductor material should be inexpensive and abundant. The bandgap edges should align with the water redox potential, and the material should also be chemically stable under illumination in an aqueous solution. Following the discovery by Fujishima and Honda in 1971 [42], that $H_2$ and $O_2$ could be produced from water splitting by photoexcitation of crystalline $TiO_2$, a good number of metal oxide semiconductors such as $Fe_2O_3$, $Ga_2O_3$, and $In_2O_3$, have been extensively investigated for water splitting applications [43–46].

Generally, metal oxides have been considered excellent materials in water-splitting reactions due to their catalytic activity, nontoxicity, high chemical stability, and low cost [47]. However, the wide bandgap of these materials has limited their visible light absorption such that the solar conversion efficiency of oxide thin films is too low for commercial application. Whereas the bandgap energy of metal sulphide semiconductors is low and suitable for visible light harvesting. They photocorrode easily in aqueous solutions [48], the oxide semiconductors are stable under solar illumination. Therefore, it is essential to improve the metal oxide photoelectrodes' solar energy conversion and charge-carrier transport properties [49]. Commonly, metal ion doping [50–53] and compound synthesis of semiconductor systems (Ti-$Fe_2O_3$/$Cu_2O$) [54] have been employed in engineering the bandgap of the oxides to enhance their visible light absorption and also improved their photocurrent generation capability. However, a lot still needs to be done.

## 1.2 Problem Statement

CVD technique is a convenient and facile synthesis method with different parameters that could be varied to fabricate $In_2O_3$ nanostructures with good crystallinity. The growth ambient plays a vital role in determining the materials' properties. Due to the low evaporation pressure of indium, synthesis is mostly performed in inert, mildly reducing and oxidizing ambient at high pressure and high temperatures. However, synthesis of high yield $In_2O_3$ nanostructures can be achieved at atmospheric pressure under strong reducing ambient like hydrogen [1].

The use of a seed layer is known to enhance material growth in the CVD synthesis technique. Commonly, gold (Au) has been widely employed as a catalyst layer in the fabrication of $In_2O_3$ nanostructures. However, the CVD growth of $In_2O_3$ nanostructures using less expensive metal catalyst as nickel (Ni) has not been well reported in the literature. There is therefore, the need to investigate the growth and physical properties of $In_2O_3$ films using Ni catalyst, for more understanding of its properties and enhanced practical applications.

Carrier gas flow rates greatly influence the morphology of $In_2O_3$ nanostructures synthesized by the CVD method. Argon (Ar) gas has been used as a carrier gas in most CVD synthesis of $In_2O_3$ nanostructures. Though various $In_2O_3$ nanostructures with exciting properties for device applications have been achieved using Ar as a carrier gas, investigation of material properties is a work in progress. The use of 1 % $H_2$ balance $N_2$ as a forming/carrier gas for the CVD growth of $In_2O_3$ nanostructures may offer an alternative for synthesizing novel nanostructures with potential device applications.

$In_2O_3$ is an important candidate for the direct photocatalysis of water splitting. With low resistivity and excellent chemical stability, its bandgap edges bracket the

redox potential of water [55–57]. However, like other oxide semiconductors, the wide bandgap (3.75 eV [58,59]) limits its utilization of visible light such that the overall solar energy harvesting efficiency is very low. Although the bandgap of $In_2O_3$ has been recently reported to be ≈ 3.0 eV [60], the absorption is low [61]. $In_2O_3$ bandgap engineering through metal ion doping, creation of O deficiency in the $In_2O_3$ lattice structure and compound synthesis of $In_2O_3$ films has been reported to improve its solar absorption and enhanced photoactivity for water splitting; however, further improvement in the solar conversion efficiency of the material is still needed [30,62–68]. The development of $In_2O_3$ based photoelectrodes by CVD technique under hydrogen reducing ambient and N-doping of the $In_2O_3$ based photoelectrodes fabricated by the CVD method may be a possible way of engineering its bandgap to achieve full utilization of visible light spectrum for hydrogen generation.

## 1.3 Research Objectives

The following objectives have been advanced to carry out this study:

i. To study morphological, structural, and optical properties of $In_2O_3$ nanostructured films synthesized on p-type (100) Si substrates by hydrogen reducting chemical vapor deposition (HRCVD) method at different growth temperatures and investigate the PEC activity of the $In_2O_3$-based photoelectrodes.

ii. To investigate the effect of deposition temperature and gas flow rate on the morphological, structural, and optical properties of $In_2O_3$ nanostructures grown on nickel-coated p-type (100) Si substrates by carbothermal reduction of $In_2O_3$ powder.

iii. To evaluate the effect of ammoniation duration on the morphological, structural, and optical properties of $In_2O_3$ nanostructured materials prepared by a simple CVD method and investigate the photoanodic performance of nitrogen-doped, $In_2O_3$ based-photoelectrodes developed by annealing $In_2O_3$ films under ammonia flow for different durations.

## 1.4 Originality of Research

The novelty of this research work lies in the following points:

i. The synthesis of $In_2O_3$ nanostructures by CVD technique under hydrogen ambient at atmospheric pressure and investigation of their photoelectrodes for PEC activity.

ii. The fabrication of high yield $In_2O_3$ nanostructures on Ni/Si by carbothermal reduction of $In_2O_3$ powder using 1 % $H_2$ balance $N_2$ as a carrier gas for the first time.

iii. The development of N-doped $In_2O_3$ nanostructures by the CVD process and the fabrication of N-doped $In_2O_3$ based photoelectrodes for photoelectrochemical application.

## 1.5 Scope of the Study

This research work will focus on the synthesis of $In_2O_3$ nanostructured films on p-type Si(100) and p-type Ni/Si(100) substrates by using chemical vapor deposition technique at atmospheric pressure under hydrogen reducing ambient, and carbothermal reduction, respectively, and to study their surface morphology, crystal structure, and optical properties. The growth of $In_2O_3$ films on p-type $Si_{(100)}$ has been performed under a hydrogen reducing environment. The growth temperature has been

optimized by varying the deposition temperature from 700 – 1050 $^{o}$C. The optimal growth temperature ranges from 900-1050 $^{o}$C were considered for reporting based on the morphological analysis. Synthesis of $In_2O_3$ films on p-type Ni/Si(100) substrates by carbon reduction was then carried out at the same temperature range. The influence of gas flow rates and N-doping through post-annealing under ammonia flow for different time intervals were also investigated. Furthermore, photoelectrodes were then fabricated based on conditions for $In_2O_3$ films deposited on Si substrates under hydrogen ambient and that for the N-$In_2O_3$ and applied in photoelectrochemical studies.

## 1.6 Thesis outline

This research has been divided into six chapters as follows:

Chapter 1 is dedicated to the introduction of the research topic. The problem statement, research objective, and originality of research are all presented in this chapter. Chapter 2 deals with a literature review on the structural, optical, and electrical properties of $In_2O_3$ nanostructures. The principle of vapor route growth mechanism of nanostructures and a review of previous works on $In_2O_3$ crystals growth for electrochemical applications. The theory of photoelectrochemical reactions and the basic principle in photocatalytic water splitting is discussed in this chapter. Chapter 3 concerns the methodology and instrumentations used in the preparation of $In_2O_3$ nanostructures and device applications. Chapter 4 deals with results and discussions of $In_2O_3$ nanostructured films synthesized via hydrogen and carbothermal reduction processes on Si and Ni/Si substrates using a horizontal tube furnace at different growth conditions. Chapter 5 discusses the results of N-doped $In_2O_3$ nanostructured films synthesized at different ammoniation durations. The chapter also presents and

discusses the investigation of the PEC performance of N-doped $In_2O_3$ based photoelectrodes. The PEC measurement for the photoanodes was carried out in a 0.5 M KOH aqueous solution. In Chapter 6, some critical remarks and suggestions for complementary and future research studies are presented in this chapter.

# CHAPTER 2

# LITERATURE REVIEW AND THEORETICAL BACKGROUND

## 2.1 Introduction

This chapter presents a brief review of the growth and fundamental properties of indium oxide. The techniques used by many groups for synthesizing $In_2O_3$ films have been discussed. A quick overview of the synthesis of $In_2O_3$ films by CVD is also presented in this chapter. A highlight of the application of $In_2O_3$ films with particular attention on photoelectrochemical studies is also given in the chapter. Furthermore, a brief review of the theoretical background of some critical concepts involved in data collection and analysis is also presented in this chapter.

## 2.2 Overview on $In_2O_3$ Growth

Indium oxide ($In_2O_3$) is an attractive, transparent semiconducting oxide (TSO) that has been studied for decades. However, after a brief investigation into its semiconducting properties, most effort has been targeted toward its numerous application as the transparent conducting oxide (TCO) indium-tin-oxide and, to a lesser extent, as an active gas-sensor material. The rediscovered of $In_2O_3$ and related TSOs as true wide-bandgap materials in the last two decades has been rigorously studied from the standpoint of semiconductor physics. According to Bierwanen [69], most $In_2O_3$ research began more than 65 years ago, when Rupprecht G. in 1954 discovered that oxidizing an evaporation-deposited indium layer at high temperatures in air produced polycrystalline $In_2O_3$ that was transparent and conductive. Its conductivity was affected by the oxygen content of the surrounding environment at high temperatures and changed in a vacuum when illuminated. These experimental

results form the foundation for the current use of $In_2O_3$ as an active layer in gas sensors, with conductivity [70] or Seebeck coefficient [71] that are highly dependent on the gas ambient in contact with the $In_2O_3$. Polycrystalline films made of nm-sized single-crystalline $In_2O_3$ grains are currently used as sensing materials [72], while single-crystalline nanowires [18] are proposed and explored. These geometries have a high aspect ratio, which rationalizes the influence of surface chemistry on surface band bending (depletion zones or accumulation layers) as an underlying mechanism influencing carrier conductivity, Seebeck coefficient, and concentration.

About 60 years ago, Groth [73] demonstrated that doping $In_2O_3$ with a few atomic % of Tin strongly increases electron concentration to multiple $10^{20}$ $cm^{-3}$, leading to unexpectedly high conductivity and infrared reflectivity while retaining high transparency in the visible region. Premised on this discovery, TCO Tin-doped $In_2O_3$, also known as indium-tin-oxide (ITO), found its primary applications in transparent contacts for flat panel displays [64], windows coatings, transparent current spreading layers in light-emitting diodes [74], solar cells [75], infrared-reflective [76] and electrochromic [77] and cladding layers for InGaN-based lasers etc.

## 2.2 Fundamental Properties of $In_2O_3$

Indium oxide belongs to the family of rare earth sesquioxides ($R_2O_3$) materials. Reports from the literature indicate that it crystallizes in three forms: the rhombohedral (corundum type) and two body-centred cubic (bcc) phases (bixbyite type) $I2_13$ and Ia3 [78]. The $I2_13$ cubic phase is unstable and can quickly transform into the Ia3 phase under a slight variation in pressure or temperature. It is therefore regarded as a distorted form of Ia3 $In_2O_3$ [79,80]. The rhombohedral polymorph is also less stable compared to Ia3 cubic; when heated at high temperatures (> 500 $^oC$), it transforms

irreversibly into the cubic Ia3 $In_2O_3$ [70] [22,79,81]. The rhombohedral phase is therefore tricky to synthesise due to its structural instability. Hence, in this work, only the cubic Ia3 phase will be considered.

The structure of $In_2O_3$ is made of 80 atoms per supercell, 32 metallics, and 48 oxygen atoms, according to the 2/3 (cation/anion) composition ratio. There are eight fluorites–type unit cells in a given supercell, consisting of two indium sites (In-b site and In-d site) with different symmetries. There are eight (8) In atoms in the b site and 24 In atoms in the d site. The crystal is stacked with three different layers along the (001) direction. The D-layer consisting of only In-b atoms, M-layer is made up of both In-b and In–d atoms. Oxygen layers separate the D and M layers (denoted as O-layer) and 48 oxygen atoms in the e-site, based on Wyckoff's notation [71,72]. The schematic of the $In_2O_3$ crystal structure is shown in Figure (2.1).

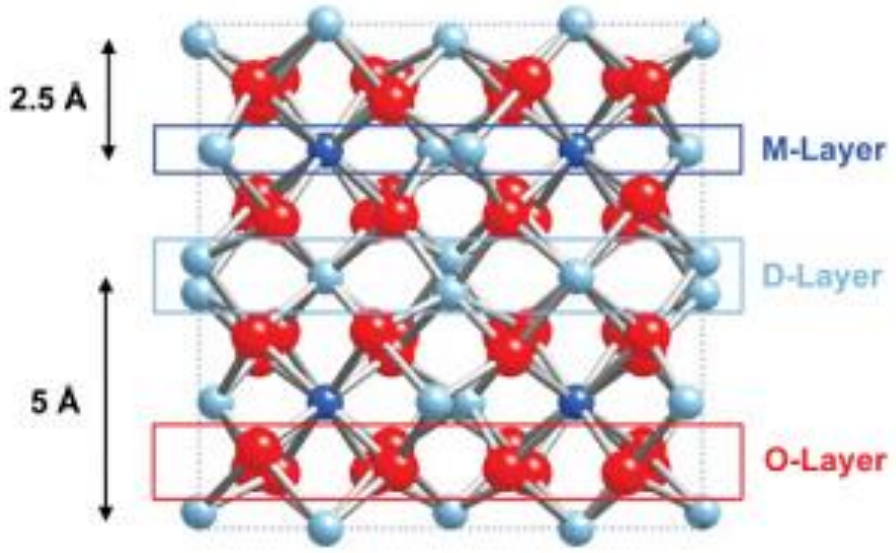


Figure 2.1: (Color online) Unit cell of the $In_2O_3$ bixbyite structure. Large (red/dark grey) balls are oxygen, and small blue balls are In-b (medium grey) and Ind (light grey). (Figure adapted from [83])

Experiments have shown that, when prepared at low substrate temperatures (≤ 250 $^oC$), $In_2O_3$ exhibits an amorphous nature; a cubic crystalline structure with

preferential growth in the (222) plane is, however, formed when synthesized or annealed at high temperatures (>250 $^{o}$C). The cubic structure of $In_2O_3$ is maintained even when the films are prepared at very high substrates temperatures or with high doping concentrations of say (Fe: 50%) [11,84]. Its films can easily be formed on different substrates such as Si, glass, quartz, etc. [5]. Theoretical and experimental investigations have shown that due to different symmetry sites, indium oxide with two kinds of sites occupied preferentially by magnetic doping will exhibit difference in magnetic properties [8,85,86].

Because of the widespread use of $In_2O_3$ (mainly Tin (Sn)-doped known as ITO) as a transparent contact material in light-emitting diodes, liquid crystal displays, photovoltaic devices, and in gas sensors for the detection of $O_3$, $H_2$, and $NO_2$, [25] Most of its physical properties have been thoroughly studied. $In_2O_3$ is known to have a density and melting point of 7.18 g/cm$^3$ and 1912.0 $^{o}$C, respectively (107). A thermal capacity of 99.01 J/Kmol at 300 K [87], a thermal expansion coefficient of 7.20 ±0.06 1/K (108), the refractive index in the visible range of 2.0±0.1 [88], and permittivity of 4 [89] are also reported in the literature.

Despite the wide application of $In_2O_3$ as transparent conducting oxides (TCOs), its bandgap structure had been a subject of intense debate over time. It has long been reported to have a direct optical band gap of about 3.75 eV from the onset of significant absorption, with a low-intensity onset of absorption below this energy attributed to indirect optical transition [90,91]. However, theoretical calculations found no significant indirect nature of the bandgap, contradicting the indirect bandgap hypothesis [58,80]. Recently, there has been a reconciliation between experimental and theoretical calculations indicating $In_2O_3$ to have a direct optical bandgap of ≈3.0

eV [80,92–94]. According to King et al. [59], the weak optical absorption around the bandgap can be ascribed to transitions between the valence-band maximum (VBM) and the conduction-band minimum (CBM) being dipole forbidden or having only minimal dipole intensity.

Many factors influence the electrical properties of $In_2O_3$ films. Depending on the preparation method and growth parameters, metallic, semiconductor or insulating $In_2O_3$ films may be obtained. Some factors include substrates temperature, doping concentration, post-deposition heat treatment and film thickness [5,24,95]. Studies have shown that thin-film sheet resistance is directly proportional to thickness. Charge carrier mobility has also been reported to increase with increasing substrate temperature, thereby enhancing electrical conductivity [96].

The oxidation state of indium governs electrical conductivity in un-doped $In_2O_3$ films. Rather than the stoichiometric structure $(In^{3+})_2(O^{2-})_3$, oxygen vacancy ($V_0$) creates a sub-stoichiometric or nonstoichiometric structure. The defect chemistry is usually employed to explain the conductivity mechanism for the indium oxide system. When there is a high concentration of $V_0$, an impurity band created by $V_0$ is formed to overlap the bottom of the conduction band, resulting in a degenerate semiconductor. The sub-stoichiometry for an intrinsic indium oxide film is given by the expression (2.1);

$$In_2O_{3-V}(V_0)ye'2y \tag{2.1}$$

where $y$ is the number of doubly charged oxygen vacancies ($V_0$) which is usually less than 1%, depending on the oxidation state, and $e'$ represents the electrons needed for charge neutrality. Non-stoichiometry in an oxide material may be regarded

as point defects in the crystal lattice structure compared to stoichiometric conditions. When non-stoichiometry in oxide is due to oxygen deficiency, the dominant defects in the material may be either oxygen deficit or interstitial metal ions, or both. The formation of both oxygen vacancies and interstitial cations leads to the formation of complimentary free electrons given rise to n-type conductivity in the material. In indium oxide films, oxygen deficiency is considered to be equivalent to the presence of excess indium compared to the stoichiometric composition. In which case, the interstitial $In^{+3}$ are the dominant defects. The contribution of the $In^{+3}$ to the conductivity is, however, known to be below 0.1 %. Hence it is not taken into account. Therefore, the significant contribution to conductivity in an $In_2O_3$ film is oxygen vacancy [97–99].

Apart from $V_0$, dopant elements with four more valence electrons can generate electrons in $In_2O_3$ films. The use of metals like Ge, Sn, Te, S, Zn, and F as dopants have widely been reported in the literature, the most effective been Tin (Sn). The chemical composition for un-doped indium oxide could be written as $In_2O_{3-x}$ and is regarded as a mixed conductor with electronic and ionic ($O^{2-}$) conduction [99]. The ionic contribution is, however, less significant compare to the electronic conduction. For a doped indium oxide, the chemical composition may be written as, $In_{2-x}Y_xO_{3-x}$. For effectiveness, the dopant element should have the same or less ionic radius as the host [100]. $In_2O_3$ films may act as a conductor, semiconductor, or insulator depending on the stoichiometric or doping state. For intrinsic $In_2O_3$ films, the presence of any $V_o$ state contributes to two weakly bonded free electrons in its nonstoichiometric form. Thus free carrier concentration can be enhanced with increased oxygen vacancies. However, increased carrier concentration at a higher doping level may result in deviation in the crystal structure and electron scattering at the grain boundaries, which

will increase resistivity in the film [101,102]. Table 2.1 below summarized the physical properties of $In_2O_3$.

Table 2.1 Summary of fundamental properties of indium oxide

| S/No. | Properties of $In_2O_3$ | Magnitude | Reference |
|---|---|---|---|
| 1 | Melting point | 1912 ($^oC$) | [22] |
| 2 | Molar mass | 277.64 g/mol | [22] |
| 3 | Density | 7.18 ($g/cm^3$) | [22] |
| 4 | Crystal structure | bcc | [83] |
| 5 | Space group | 206, Ia3 | [69] |
| 6 | Lattice constant | 1.0117 (nm) | [69] |
| 7 | Cell volume | 1035.51 ($Å^3$) | [69] |
| 7 | Thermal expansion | 7.20 (1/K) | [22] |
| 8 | Permittivity | 4 | [89] |
| 9 | Refractive index | 2.0 | [88] |
| 10 | Bandgap | 3.0-3.75 (eV) | [59,60] |
| 11 | Carrier type | n-type | [88,92] |
| 12 | Resistivity | $\geq 10^{-4}$ (Ω cm) | [92] |
| 13 | Carrier density | $\geq 10^{19}$ ($cm^{-3}$) | [88,92] |
| 14 | Carrier mobility | 55-95 ($cm^2$/V.sec) | [88,92] |

## 2.3 Fabrication techniques for $In_2O_3$ films

Material synthesis is of great importance in the modern era of technology for various device applications. Depending on the synthesis technique, nanostructures or thin films have unique morphological, physicochemical, and structural properties necessary for a wide range of applications in optical, optoelectronic, electronic, electrochemical, biomedical, and environmental fields. Various techniques can be

employed to produce thin and nanostructured films, which can broadly be grouped under two headings, namely, physical and chemical deposition processes. The physical deposition method is also referred to as the top-bottom technique. It is a synthesis technique that involves the condensation of vaporized material from a source species onto a substrate surface under a partial vacuum condition. Examples include thermal evaporation, chemical vapor deposition, sputtering, laser ablation and high energy ball milling. On the other hand, chemical deposition processes are bottom-up synthesis techniques that involve coalescence or assembling molecules and atoms to form a diverse range of coatings. Examples include sol-gel, spray pyrolysis, plating and chemical bath deposition (CBD) [103–105]. This section is dedicated to a brief review of some syntheses of $In_2O_3$ in the last two decades as reported in the literature by different groups. The focus will be on the type of material synthesized, growth method, substrate, precursor, dopant, morphology, and application. Structural, optical, and electrical properties of the synthesized materials will also be highlighted.

Yahia *et al*. [106] investigated the influence of molar concentration on $In_2O_3$ thin films grown by a sol-gel spin coating method using indium (III) nitrate hydrate, ethanol, and acetylacetone as source materials. Films were observed to be homogenous, uniform and dense surfaces. The roughness of the films was observed to increase with increased molarity. Increased surface roughness was ascribed to a change in the surface structure of films due to the appearance of a new growth direction. Fechete and co-workers.[107] reports the synthesis of $In_2O_3$ nanostructures by thermal evaporation method on Si substrates with and without a gold catalyst at reduced ambient. $In_2O_3$ powder was used as the source material, and the growth temperature was varied between 600-900 $^oC$. Their result revealed the formation of nanobelts with different widths at 750 $^oC$ when no catalyst was used. In comparison, homogenously

scattered nanorods were obtained at 900 $^{o}$C with the use of a gold catalyst. CVD synthesis of 1-D single-crystal $In_2O_3$ nanobouqets, nanowires, nanopowders and nanocones on Au/Si substrates for super capacitive application was reported by [108]. The effect of deposition temperature on the properties of the films was studied by varying the temperature between 600-1000 $^{o}$C. The nanostructures were found to grow through VLS and LS mechanisms depending on the source temperature. Films morphology was also observed to be temperature-dependent.

Hatem *et al.* [2] fabricated titanium-doped indium tin oxide thin films on glass substrates using the sol-gel spin coating technique. Morphological, structural, optical, and electrical properties of the Ti-ITO films were investigated by varying the concentration of Ti from 0-4% and annealing temperature from 150-600 $^{o}$C. The crystallinity of the material was observed to increase with increasing Ti ratio as well as annealing temperature. Increased annealing temperature also enhanced the electrical and optical properties of the films. Indium oxide and molybdenum-doped indium oxide (IMO) thin films were synthesized on a glass substrate via spray pyrolysis using $InCl_3$ as precursor and $MoCl_5$ as a dopant. The deposition temperature and dopant concentration were observed to influence the films' structural, optical, electrical and morphological properties [109]. Sen *et al*. [110] synthesized hydrogen doped indium oxide ($In_2O_3$:H) for silicon heterojunction solar cell application by a DC magnetron sputtering technique. A comparative investigation of the physical properties revealed that the $In_2O_3$:H films have lower carrier density, higher Hall mobility, and a broader transmittance range for optimized $O_2$ and $H_2$ flow rates than traditional ITO films. Carrier concentration and Hall mobility for the $In_2O_3$:H films increased with increasing $H_2$ flow rate during the growth process. This unusual observation was attributed to the

mechanism that hydrogen impurities induced some shallow donors in the $In_2O_3$:H, which have a low scattering effect on carrier transport.

Jolanta *et al*. [111] report synthesis of $In_2O_3$ thin film on various substrates (Fused-quartz, GaAs, &Si(100) ) by pulsed laser deposition (PLD) under different oxygen gas pressures, using ceramic $In_2O_3$ target as source material. The films were highly transparent. A drastic change in morphology and electrical resistivity of the films with increased $O_2$ pressure into mbar range was observed. The ion beam assisted deposition (IAD) technique was used to prepare $In_2O_3$ thin films on indium phosphide (InP) substrates. By varying the ambient oxygen pressure during the growth process, $In_2O_3$ films with low optical loss at the 1550 nm wavelength range and good conductivity were obtained [112]. Elam *et al*. [113] grew $In_2O_3$ films by atomic layer deposition (ALD) method using cyclopentadienyl indium (InCP) and combination of both molecular $O_2$ and $H_2O$ as the co-reactants. No growth was observed when $O_2$ and $H_2O$ were used alone. However, film growth was achieved at a growth rate of 1.0-1.6 Å/cycle over the full range of the deposition temperatures from 100-250 $^oC$ when $O_2$ and $H_2O$ were applied sequentially or together. The obtained films were highly transparent. Both crystallinity and electrical properties of the $In_2O_3$ films were dependent on deposition temperature and co-reactant sequence.

Du *et al*. [114] successfully prepared high-quality $In_2O_3$ films by the metal-organic chemical vapour deposition (MOCVD) method. Synthesis was performed at growth temperatures between 570-690 $^oC$ using the a-plane sapphire [$Al_2O_3$(110)] as substrate. The film synthesized at 650 $^oC$ was revealed to exhibit the best crystalline quality with no domain structures. The films also had the highest Hall mobility with the lowest resistivity and carrier concentration. All the films showed excellent transparencies in the visible region with an average transmittance of over 83 %. $In_2O_3$

nanocubes were synthesized by the hydrothermal technique using indium nitrate ($In(NO_3))_3.4H_2O$ and urea ($CH_4N_2O$) as reagents. Characterization revealed the prepared material to be single-phase $In_2O_3$ nanocubes having a smooth surface with a surface size of about 180-200 nm in width. Investigation of gas sensing properties of the nanocubes revealed a pretty high response of 12-10 ppm of trimethylamine (TEA). The morphology and sensing stability of the nanocubes were maintained even after consecutive testing for two months [115].

Aziz and co-workers [116] prepared tin-doped indium oxide nanoparticles by a hydrothermal technique using pamoic acid ($Na_2PA$) as an organic additive, $In(NO_3)_3.4H_2O$, and $SnCl_2.2H_2O$ as indium and tin precursor, respectively. Morphological analysis revealed the material to be homogeneous in shape and size. The synthesized ITO-NPs also showed high emission intensity with a peak centered at 393 nm. Yoon *et al*. [117] synthesized $In_2O_3$ microcubes for solar water splitting application. The microcubes films were prepared by the chemical bath deposition (CBD) technique using $In(NO_3)_3$ and urea as source materials, and ITO-coated glass slides were used as substrates. The effect of deposition time on the growth of the $In_2O_3$ microcubes was investigated by varying the deposition time between 2-48 h. 24 h was determined as the optimal deposition time, and the corresponding film generated a maximum photocurrent density of 0.55 $mAcm^{-2}$. Nanni *et al.* [118] reported on the synthesis of molybdenum doped indium oxide (IMO) by sol-gel dip-coating method on the soda-lime glass as a substrate. The precursor solution for the growth of the IMO films was prepared from different reagents as In and Mo sources, respectively, including either; indium nitrate hydrate $(In(NO_3)_3).H_2O$ and ammonium molybdate tetrahydrate ($(NH_4)_8Mo_7O_{24}.4H_2O$) or indium trichloride ($InCl_3$) and molybdenum pentachloride ($MoCl_5$) or indium nitrate hydrate $(In(NO_3)_3.H_2O)$ and $MoCl_5$. The

influence of reagent type, solvent and annealing ambient (air and $N_2$) on the properties of the synthesized films were investigated. It was found that film prepared using indium nitrate and molybdenum chloride performed better in morphology, crystallinity and optical transmittance.

$In_2O_3$ thin films were synthesized using reactive (RF) sputtering process using pure indium target as a precursor, and oxygen as reactive gas with argon. The properties of the films were studied by varying the chamber's pressure and gas flow rates during the growing procedure. The deposition rate was observed to increase with increasing system pressure and oxygen flow rates [119]. Seiler *et al*. [120] prepared $In_2O_3$ thin films via the pulsed electron beam deposition (PED) technique on c-cut sapphire substrates. The growth temperature was varied between 200 to 500 $^oC$. Two different structural phases were obtained in the films: the ordered bixbyite phase with the three-fold symmetry in the (111) plane and a disordered bixbyite phase with a six-fold symmetry in the (111) plane. This observation was attributed to the specificities of the growth condition, inducing a large disorder in the oxygen network.

Table 2.2 Summary of review of synthesis of $In_2O_3$ films

| Material | method | substrate | Precursor | Morphology | Application | Ref. |
|---|---|---|---|---|---|---|
| $In_2O_3$ | SGSC | Glass | $In(NO_3).xH_2O$ | Thin film | Nil | [106] |
| $In_2O_3$ | TE | Si&Au/Si | IO-powder | NR & NB | Nil | [107] |
| $In_2O_3$ | CVD | Au/Si | IO-powder | NT & NQ | Supercap. | [108] |
| Ti-ITO | SGSC | Glass | $In(NO_3).5H_2O$ | Thin film | Nil | [2] |
| IMO | SP | Glass | $InCl\&MoCl_3$ | Thin film | Nil | [109] |
| $In_2O_3$:H | DC-S | Glass | IO-target | Thin film | Solar cell | [110] |
| $In_2O_3$ | DC-S | FQ,GA,Si | IO-target | Thin film | Nil | [111] |
| $In_2O_3$ | IAD | InP | IO-target | Thin film | Nil | [112] |
| $In_2O_3$ | MOCVD | $Al_2O_3$ | TMI | Thin film | Nil | [113] |
| $In_2O_3$ | HT | Nil | $In(NO_3)_3.4HH_2O$ | NC-NPs | Gas sensing | [115] |
| ITO | HT | Nil | $In(NO_3).xH_2O/SnCl$ | NP | PL | [116] |
| $In_2O_3$ | CBD | ITO-glass | $In(NO_3)_3$+Urea | MC | W-splitting | [117] |
| IMO | D-coating | Glass | $InNO/InCl_3$/AMHO | Thin film | Nil | [118] |
| $In_2O_3$ | Sputtering | Glass | In-target | Thin film | Nil | [119] |
| $In_2O_3$ | PED | Sapphire | | Thin film | Nil | [120] |

**Notes:** -AMHO-$(NH_4)_8Mo_7O_{24}.4H_2O$, CBD-chemical bath deposition, DC-S-DC sputtering, HT-hydrothermal, IAD-ion beam assisted deposition, IMO-molybdenum-doped $In_2O_3$, InNO-$In(NO_3)_3.xHH_2O$, IO-indium oxide, MC-microcubes, NB-nanobelts, NC-nanocones, NPS-nanoparticles, NQ-nanobouqets, NR-nanorods, NT-nanotowers, PED-pulsed electron beam deposition, PL-photoluminescence, PLD-pulsed laser deposition, SGSC-sol-gel spin coating, SP-spray pyrolysis, TE-thermal evaporation, TMI-trimethylidium, W-splitting-water splitting,

### 2.3.1 Overview of solid-to-vapor deposition of $In_2O_3$ films

Solid-to-vapor deposition (SVD) commonly known as chemical vapor deposition (CVD) may be defined as the deposition of a solid on a heated surface from

a chemical reaction in the vapor phase. It belongs to the class of vapor transfer processes which is atomistic in nature, that is the deposition species are atoms or molecules or a combination of these. Besides CVD, they include various physical vapor deposition (PVD) such as evaporation, sputtering, molecular beam epitaxy (MBE), and ion plating. In this work, the CVD technique was used in preparing the $In_2O_3$ films. The CVD technique was chosen because of the targeted application since photoelectrochemical study for water splitting of CVD fabricated $In_2O_3$ electrodes have not been given much attention. The CVD is a facile synthesis method, films prepared from it are highly crystalline and have a large surface area, two important properties for photocatalytic materials. While the principle of material growth in the CVD technique is presented in Appendix I, a review on some vapor route synthesized $In_2O_3$ films is presented in this section.

Fekete *et al*.[107] reports the synthesis of $In_2O_3$ nanostructures by thermal evaporation method on Si substrates with and without a gold catalyst at reduced ambient. $In_2O_3$ powder was used as the source material, and the growth temperature was varied between 600-900 $^oC$. Their result revealed the formation of nanobelts with varying width at 750 $^oC$ when no catalyst was used, while homogenously scattered nanorods were obtained at 900 $^oC$ with the use of gold catalyst. A controlled synthesis of $In_2O_3$ nanowires on single-crystal substrates catalyzed with gold, using the CVD technique under a pressure of 100 mbar, was reported by Vomiero *et al*. [121]. Their quantitative investigation on the nucleation and growth of the indium oxide nanowires demonstrates that two competitive mechanisms concur to nanowire growth: direct VS and catalyst-mediated VLS adsorption of volatiles. VS mechanism regulates the lateral enlargement of the nanowires, which is a thermally activated process, while VLS or VS mechanisms are responsible for wire elongation, depending on the condensation

temperature. $In_2O_3$, ITO and $SnO_2$ nanostructures were grown on Au/Si and Au/quartz substrates using vapour deposition method under controlled pressure and various deposition temperatures. A mixture of metal oxide nanoparticles and carbon nanotubes was used as the precursor. The morphology and composition of the nanostructures were found that dependent on the temperature of the substrates [12].

Qurashi *et al*. [122] synthesized $In_2O_3$ nanowires and nanoneedles by chemical vapor deposition on Au/Si substrates. They revealed that reaction temperature has a profound effect on the shape and morphology of $In_2O_3$ nanostructures. Their investigation also shows that the functionality of hydrogen gas sensors fabricated from the $In_2O_3$ nanostructures was morphological dependent. The $In_2O_3$ nanowires showed better gas sensor response compared to the $In_2O_3$ nanoneedles. High-purity $In_2O_3$ nanowires have been grown without catalysts, directly from metallic indium by a vapor transport technique and a controlled oxidation with oxygen–argon mixtures. Depending on the growth parameters (temperature, vapor pressure, oxygen concentration), different results have been achieved, and it has been observed that a 'proper' In condensation on the substrates can play the role of 'self-catalyst' and allows for easy formation of the nanowires [123]. Singh *et al*. [29] synthesized Indium oxide nanowires, nanotowers and ultra-long layered nanorods through carbothermal reduction of $In_2O_3$ powder on Au/Si substrates by varying the source temperature in a CVD horizontal furnace. The growth of one-dimensional $In_2O_3$ nanostructure with diverse structures was ascribed to the alternation in growth mechanism between VLS and VS from a single precursor with the confinement of vapor pressure.

Indium oxide nanowires have been grown via carbothermal reduction using a vapour-liquid-solid mechanism on Au/Si substrates inside a chemical vapor deposition (CVD) furnace. A study of the gas sensing properties of the $In_2O_3$ nanowires revealed